A SYSTEMATIC ANALYSIS OF CAVITY COMPENSATIONS IN THE JAEA-ADS LINAC UTILIZING THE LIGHTWIN TOOL

B. Yee-Rendon*, Y. Kondo, J. Tamura, S. Meigo, and F. Maekawa,
Japan Atomic Energy Agency, Tokai Mura, Japan
A. Plaçais, and F. Bouly, Univ. Grenoble Alpes, CNRS, Grenoble INP, LPSC-IN2P3, Grenoble, France

Abstract

The Japan Atomic Energy Agency (JAEA) is designing a 30-MW linear proton accelerator (linac) for the Accelerator-Driven Systems (ADS) to address the nuclear waste storage challenges. For Accelerator-Driven Systems (ADS) technology to be viable, it is necessary to minimize both the number of beam trips and their duration, thereby exceeding the performance of current linacs. JAEA is focused on implementing fast cavity compensation to minimize beam downtime caused by cavity failures. This approach makes rapid cavity retuning that enables a fast beam restoration with an acceptable quality. Beam dynamics studies for the JAEA-ADS linac have shown that it is possible to achieve a proper beam operation even when multiple cavity failures occur. As the JAEA-ADS linac consists of 293 superconducting cavities, it requires a rapid, automated, and systematic approach to determine the optimal readjustment settings for all cavities. To achieve this, we are utilizing the LightWin tool. This software has been developed for ADS linacs and was successfully applied to ADS MINERVA/MYRRHA linac. It has undergone testing and enhancements to improve SPIRAL2 operation. This study analyzes cavity compensation in the JAEA-ADS superconducting linac using the LightWin tool and compares the results with previous research.

INTRODUCTION

As part of the research and development activities for Accelerator-Driven System (ADS) in the Japan Atomic Energy Agency (JAEA), we are doing R&D on superconducting linear accelerator (linac) to accelerate a 30-MW proton beam to generate spallation neutrons for an 800-MW thermal power subcritical reactor [1]. Table 1 presents the main characteristics of the JAEA-ADS linac [2].

Table 1: Main Parameters for the JAEA-ADS linac

Parameter	Value
Beam current [mA]	20
Proton beam energy [GeV]	1.5
Duty factor (%)	100 (cw)
Beam loss [W/m]	<1

Figure 1 shows the scheme of the JAEA-ADS linac. The JAEA-ADS linac adopts a hot standby scheme in the low-energy section and fast element compensation in the high-energy section to meet stringent reliability and availability requirements for ADS [3]. Previous studies [4–6] have shown that cavity compensation can be implemented with acceptable beam quality in the JAEA-ADS linac. However, those studies focused on the most challenging scenarios, leaving the analysis of all cavities in the high-energy section pending. Additionally, the configuration schemes differ across cavity sections, making it difficult to prepare suitable compensation schemes for all the cavities and complicating its implementation in real-world operations [7]. This study aims to address these challenges by applying cavity compensation throughout the entire high-energy section and identifying a general cavity compensation configuration that could be effective for most of the cases.

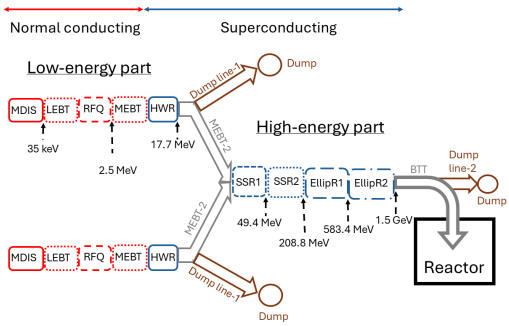

Figure 1: Layout of the JAEA-ADS linac.

JAEA-ADS LINAC: HIGH-ENERGY PART

The high-energy section accelerates a 20-mA proton beam from an initial energy of 17.7 MeV to a final energy of 1.5 GeV. This region includes four cavity sections: two single-spoke resonators sections operating at 324 MHz (SSR1 and SSR2) and two five-cell elliptical cavities operating at 648 MHz (EllipR1 and EllipR2). A summary of the relevant parameters is shown in Table 2. The total number of cavities is 268.

Table 2: Cavity parameters for the high-energy part of the JAEA-ADS linac

Section	SSR1	SSR2	EllipR1	EllipR2
Final energy (MeV)	49.4	208.8	583.4	1500
Frequency (MHz)	324	324	648	648
β_g	0.16	0.43	0.68	0.89
# of cell	2	2	5	5
Cavities per cryomodule	2	3	3	5
# of cavities	66	72	60	70

The Accelerating gradient (E_{acc}) and the synchronous phase (ϕ_s) were tuning to ensure enough longitudinal acceptance for cavity compensation, Fig. 2.

* byee@post.j-parc.jp

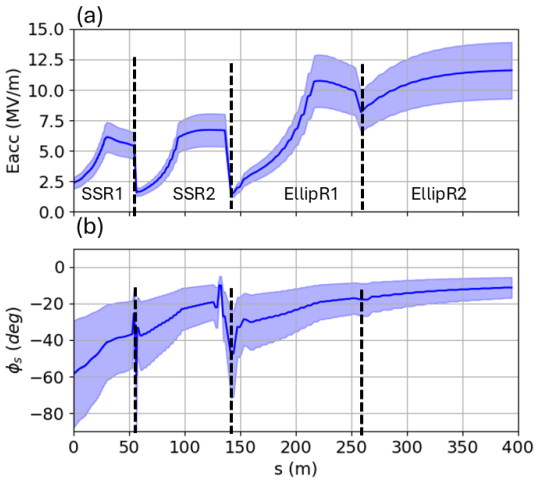

Figure 2: Accelerating gradient (a) and synchronous phase (b) along the high-energy section. The shaded region indicates the tunning range: ± 20% for E_{acc} and ±50% for ϕ_s.

CAVITY COMPENSATION PROCEDURE

The cavity compensation schemes were computed using LightWin tool [8], which is an open-source software developed in Python, compatible with the TraceWin [9] beam dynamics code. LightWin can automatically determine cavity compensation settings for several fault scenarios without requiring direct user intervention. This accelerates the creation of cavity compensation databases and facilitates the comparison of different cavity compensation schemes. LigthWin has been used in the different superconducting linacs [6, 10, 11].

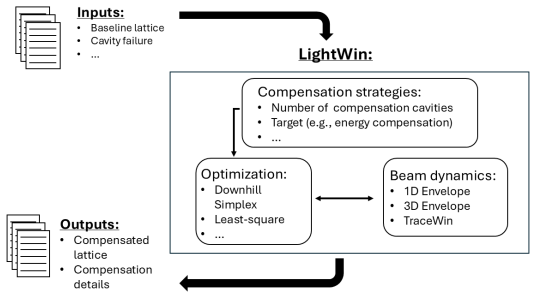

Figure 3: Simplified structure of LightWin.

LightWin consists of three main blocks: Compensation Strategy, Optimization Algorithm, and Beam Dynamics, Fig. 3 . The compensation strategy block is the most complex, as it defines the cavities that will fail, the number of cavities to be used for compensation, the optimization objectives, and the constraints associated with the adjusted parameters. In this study, the goals were to minimize the differences in beam energy, absolute phase, and longitudinal mismatch factor by readjusting E_{acc} and ϕ_s. Table 3 shows the beam performance and constraints criteria, the first five rows are the beam performance goals, and the last two rows are the constraints. The differences in energy, normalized RMS emittance (ε_{Nrms}), and mismatch factor relate to beam performance at the end of the linac, considering the baseline case. The optimization section contains various methods for adjusting the parameters to meet the desired objectives, including the Downhill Simplex, the Least Squares, among others. In this work, the Downhill Simplex method was chosen because it provides a fast and acceptable result. The beam dynamics block allows beam dynamics calculations in 1D and 3D envelope simulations, as well as multiparticle simulations using TraceWin. For this study, the beam dynamics calculations were performed on 1D envelopes and confirmed through multiparticle simulations in TraceWin.

Table 3: Beam target performance and constraints criteria. The mismatch factor is the same as defined in previous works [4, 6]

Parameter	**Value**
Total beam loss (%)	< 1
Maximum power loss (W/m)	< 1
Maximum energy difference (%)	<1
Transverse ε_{Nrms} difference (%)	30
Transverse mismatch factor (%)	0.25
Maximum retuned E_{acc} (%)	20
Maximum retuned ϕ_s (%)	50

Figure 4 shows the compensation for cavity 57, located at the 16th cryomodule of the SSR1 section. Figure 4-a presents the retuned E_{acc}, and Fig. 4-b,ϕ_s. The effect on the beam energy is displayed in Fig. 4-c.

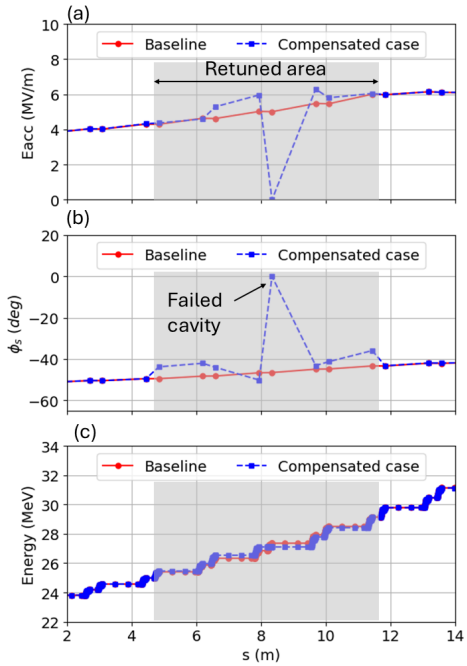

Figure 4: Comparison of the Baseline (red circle solid line) and a Compensated case (blue square dashed line). The gray area highlights the retuned area. The top and middle plot shows E_{acc} and ϕ_s of the cavities. The bottom plot shows the beam energy.

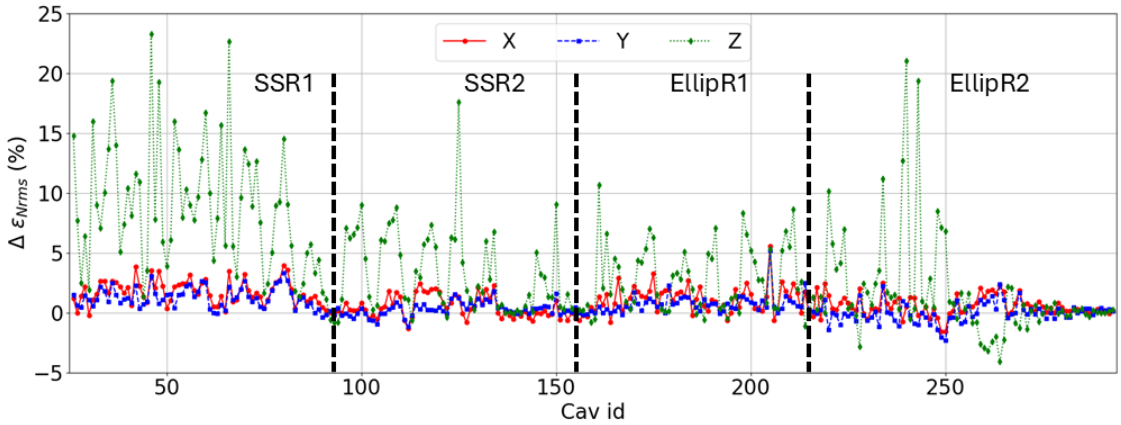

Figure 5: Deviation of the normalized RMS emittance (ε_{Nrms}) at the end of the linac with respect to the baseline as a function of the faulty cavity in the high-energy sections.

RESULTS

The analysis is center on single cavity compensation, as this represents the most likely case. Early study [4] concluded that between four to seven cavities are necessary to compensate for a single failed cavity. Thus, we decided to use seven cavities for compensation.

We did not observe beam losses in any of the 268 analyzed cases. However, seven of them reported large longitudinal ε_{Nrms} in the last section, exceeding the baseline by more than 30%. Those cases exhibited large phase drifts, affecting downstream ϕ_s . This issue could be mitigated by increasing the number of compensating cavities to nine or ten. ε_{Nrms} increase could be kept below 25%, with three cases beyond 20%. We show in Fig. 5 the change in longitudinal ε_{Nrms} with respect to the baseline for every scenario.

Figure 6 illustrates the histograms of beam energy, ε_{Nrms} growth, and mismatch factor. The centroid of the beam energy deviates from the baseline by less than 0.2%. The change on the transverse ε_{Nrms} remains within ±5%, while the longitudinal change increases to less than 25%. Negative values indicate emittance transfer between planes. Transverse mismatch factor is less than 0.2, but it increases to 0.45 in the longitudinal plane. It is worth noting that the longitudinal mismatch factor is higher compared to previous studies; however, the other beam parameters, such as longitudinal ε_{Nrms} and energy, remain similar with earlier studies. Since the following section after the linac, the beam transport to the target, does not require any longitudinal matching, we consider this performance acceptable for the ADS.

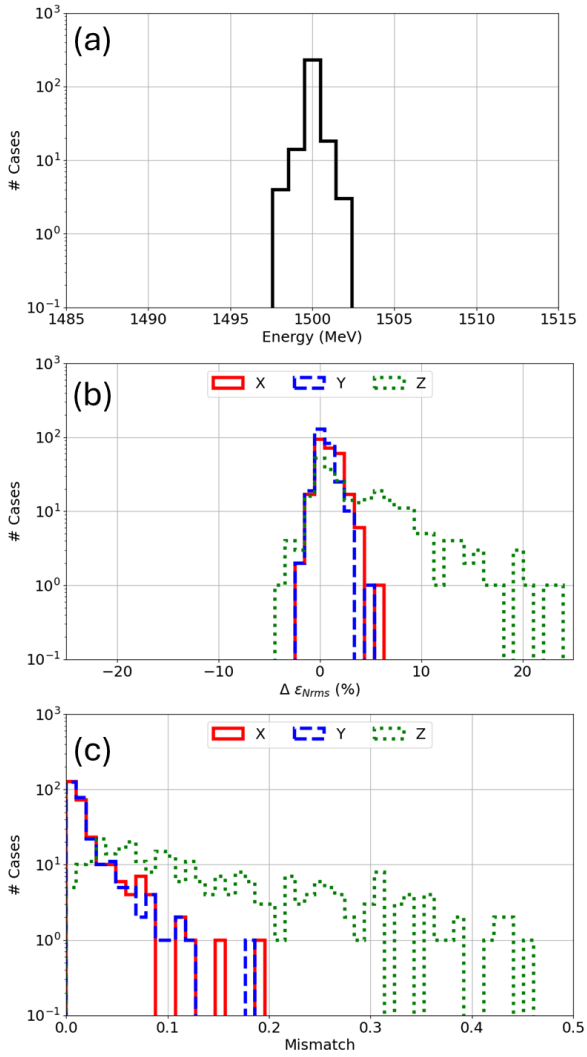

Figure 6: Histogram of the beam energy (a), change of the final ε_{Nrms}(b) and mismatch factor (c).

CONCLUSION

This work advances previous JAEA-ADS cavity compensation studies by applying cavity compensation to all cavities in the high-energy part, thereby confirming the effectiveness of this approach to ensure high availability and acceptable beam quality for the JAEA-ADS linac operation.

Furthermore, this work addresses the challenge of reducing the large number of cavity compensation configurations, demonstrating that seven cavities (four-three) are sufficient to compensate for over 97% of cases, thus reducing complexity for its future application in real-time operation.

ACKNOWLEDGMENTS

This work is supported by JSPS KAKENHI Grant Number 24H00235.

REFERENCES

[1] T. Sugawara *et al.*, "Research and Development Activities for Accelerator-Driven System in Jaea", *Prog. Nucl. Energy*, vol. 106, pp. 27, Feb. 2018. doi:10.1016/j.pnucene.2018.02.007

[2] B. Yee-Rendon *et al.*, "Design and beam dynamic studies of a 30-MW superconducting linac for an accelerator-driven subcritical system", *Phys. Rev. Accel. Beams.*, vol. 24, pp. 120101, Dec. 2021. doi:10.1103/PhysRevAccelBeams.24.120101

[3] H. Takei *et al.*, "Estimation of acceptable beam-trip frequencies of accelerators for accelerator-driven systems and comparison with existing performance data", *J. Nucl. Sci. Techol.*, vol. 49, pp. 384, Sep. 2012. doi:10.1080/00223131.2012.669239

[4] B. Yee-Rendon *et al.*, "Beam dynamics studies for fast beam trip recovery of the Japan Atomic Energy Agency accelerator-driven subcritical system", *Phys. Rev. Accel. Beams.*, vol. 25, pp. 080101, Aug. 2022. doi:10.1103/PhysRevAccelBeams.25.080101

[5] A. Plaçais, F. Bouly, and B. Yee-Rendon, "Development of a Tool for Cavity Failure Compensation in Superconducting Linacs: Progress and Comparative Study", in *Proc. IPAC'23*, Venice, Italy, May 2023, pp. 4097–4100. doi:10.18429/JACoW-IPAC2023-THPA060

[6] B. Yee-Rendon *et al.*, "Cavity compensation studies in the JAEA-ADS superconducting linac using LightWin", in *Proc. SRF2025*, Tokyo, Japan, Sep. 2025, pp. 316–320.

[7] V. S. Morozov, C. C. Peters, and A. P. Shishlo, "Oak Ridge Spallation Neutron Source superconducting rf linac availability performance and demonstration of operation restoration with superconducting rf cavity off ", *Phys. Rev. Accel. Beams.*, vol. 25, pp. 020101, Feb. 2022. doi:10.1103/PhysRevAccelBeams.25.020101

[8] A. Plaçais *et al.*, LightWin, https://github.com/AdrienPlacais/LightWin

[9] D. Uriot and N. Pichoff, "Status of TraceWin Code", in *Proc. IPAC'15*, Richmond, VA, USA, May 2015, pp. 92–94. doi:10.18429/JACoW-IPAC2015-MOPWA008

[10] A. Plaçais *et al.*, "Automatic retuning of superconducting linacs using LightWin", in *Proc. LINAC'24*, Chicago, IL, USA, Aug. 2024, pp. 563–568. doi:10.18429/JACoW-LINAC2024-THXA001

[11] A. Plaçais *et al.*, "Towards automated cavity failure compensation in the SPIRAL2 SC Linac", presented at the 17th International Particle Accelerator Conf. (IPAC'26), Deauville, France, May 2026 paper THP4019, this conference.